Pubblicazioni del Centro De Giorgi
Proceedings of the Interdisciplinary Workshop on Mathematical Methods in Biomedical Imaging and Intensity-Modulated Radiation Therapy (IMRT), Pisa, Italy, October 2007.

Image Reconstruction and Image Analysis in Tomography: Fan Beam and 3D Cone Beam

Alfred K. Louis and Thomas Weber

ABSTRACT. The result of tomographic examination is a series of images of the region under consideration. On these reconstructions a diagnosis is based. Automatic evaluations of these images are rather common in nondestructive testing, in medical analysis this may partially be the case in the future. Typically the two tasks are treated separately. This paper describes an approach where the two steps, the image reconstruction and the image analysis, are combined. This leads to new strategies how to develop fast algorithms. As example we consider the standard problem in X–ray tomography and an edge detection. We calculate a special reconstruction kernel, and we present numerical examples.

.

1. Introduction

The filtered backprojection is the standard reconstruction method for 2D X—ray tomography. Already Grünbaum [**6**] observed that this algorithm determines a smoothed version of the searched-for solution. In different fields the calculation of such smoothed versions of the solution is the starting point for developing algorithms, see e.g. [**1, 21, 16**]. A first unified approach was given in [**29**], which then was generalized in [**24**] for the application to linear and also to some nonlinear problems. In [**28**] this so-called approximate inverse was further generalized to directly

---

Key words and phrases. Image analysis, inverse problems, tomography, approximate inverse.

The authors were supported in part by the Hermann and Dr. Charlotte Deutsch Stiftung.

compute linear functionals of the solution. The calculation of derivatives for functions of one variable was already mentioned by Eckhardt, [**9**], and also, including numerical experiments, in [**24**].
In this paper we study the problem of determining $\mathbf{L}f$ where f is the solution of the linear equation $\mathbf{A}f = g$. The standard case in reconstruction problems is that the operator $\mathbf{L}$ is the identity, hence we calculate the solution itself. If we include in the solution step the evaluation of the reconstruction, then we may enhance this task by incorporating parts of the evaluation in the reconstruction. An example is edge detection where smoothed derivatives of the images are calculated and then further processed. In that case $\mathbf{L}$ may be a differential operator, which increases the degree of the ill-posedness of the whole problem. Other possibilities are the direct calculation of wavelet coefficients of the solution, as originally described in Sec. 3.4.3 in [**31**]. Applications to tomography are given in [**3, 37**].

Often, the two procedures are executed independently. If the image is itself the result of a reconstruction, for example in medical imaging, one can envisage, that the information from the reconstruction step could be included into the analysis step, which then should give better results.

As example, for a given picture f we compute partial derivatives $\mathbf{L}_k = \frac{\partial}{\partial x_k}$, hence the result can be written as

$$L_{k\beta} f = f_{k\beta} = W_\beta L_k f \tag{1.1}$$

for a smoothing operator W_β. If the image f is a reconstruction, say the solution of

$$\mathbf{A}f = g \tag{1.2}$$

we can write the solution, when filtering is considered, as

$$f_\gamma = E_\gamma f = E_\gamma \mathbf{A}^\dagger g \tag{1.3}$$

where $\mathbf{A}^\dagger$ denotes the generalized inverse of $\mathbf{A}$. Combining these two steps we get

$$\begin{aligned} f_{k\beta\gamma} &= W_\beta L_k E_\gamma \mathbf{A}^\dagger g && (1.4)\\ &= \Psi_{k\beta\gamma} g\ . && (1.5) \end{aligned}$$

There arise several questions

- is there an optimal relation between the two smoothing operators W_β and E_γ ?
- how to choose the parameters β and γ ?
- can this operator $\Psi_{k\beta\gamma}$ be efficiently evaluated ?

Concerning the last question we know that for the reconstruction step a convolution operator E_γ leads to the filtered backprojection method. Hence we are looking for similar structures in the operator W_β.

After describing the general approach of developing algorithms for calculating $\mathbf{L}f$ in Section 2 we present the special case of fan - beam tomography in Section 3 for the case where $\mathbf{L}_k$ is the differentiation of first order in the k - th coordinate direction. We then consider the standard reconstruction problem; i.e. $\mathbf{L}$ the identity, for cone - beam tomography for a circular scanning geometry.

2. Approximate Inverse for Combining Reconstruction and Analysis

This section is based on [**28**] where we generalize the method of the approximate inverse as analyzed in [**24**]. Let $\mathbf{A} : X \to Y$ be a linear operator between the Hilbert spaces X and Y and $L : X \to Z$ be a linear operator between the Hilbert spaces X and Z. As usual we first formulate the reconstruction part

$$Af = g \; . \tag{2.1}$$

Next an operation L on the so computed solution f for the image analysis is performed

$$Lf = LA^\dagger g \; , \tag{2.2}$$

where $A^\dagger$ denotes the generalized inverse of A. Now we adapt the concept of approximate inverse, first introduced in [**29**], where we now compute instead of Lf an approximation

$$(Lf)_\gamma = \langle Lf, e_\gamma \rangle$$

with a prescribed mollifier e_γ. We formulate in the following theorem the principle of the reconstruction method.

THEOREM 2.1. *Let e_γ be a suitably chosen mollifier and ψ_γ be the solution of the auxiliary problem*

$$A^* \psi_\gamma(x, \cdot) = L^* e_\gamma(x, \cdot) \; . \tag{2.3}$$

Then the smoothed version of the image analysis operation is directly computed from the given data g as

$$(Lf)_\gamma(x) = \langle g, \psi_\gamma(x, \cdot) \rangle \tag{2.4}$$

PROOF. We write the smoothed version of the image analysis part as

$$(Lf)_\gamma(x) = \langle Lf, e_\gamma(x, \cdot) \rangle$$

Now we use the adjoint operator of L and the auxiliary problem to continue

$$\begin{aligned}(Lf)_\gamma(x) &= \langle f, L^* e_\gamma(x,\cdot)\rangle \\ &= \langle f, A^*\psi_\gamma(x,\cdot)\rangle \\ &= \langle g, \psi_\gamma(x,\cdot)\rangle\end{aligned}$$

where in the last step we have used the original equation $Af = g$. □

DEFINITION 2.2. The operator $S_\gamma : Y \to Z$ defined as

$$S_\gamma g(x) = \langle g, \psi_\gamma(x,\cdot)\rangle \tag{2.5}$$

is called the *approximate inverse* of A to compute an approximation of Lf and ψ_γ is called the *reconstruction kernel*.

If we know the reconstruction kernel for computing f, then we can solve the above problem for computing Lf in the following way.

THEOREM 2.3. *Let $\tilde{\psi}_\gamma$ be the sufficiently smooth reconstruction kernel for computing f, then the reconstruction kernel ψ_γ for approximating Lf can be determined as*

$$\psi_\gamma = LW_\beta \tilde{\psi}_\gamma \tag{2.6}$$

where LW_β acts on the first variable of $\tilde{\psi}_\gamma$.

PROOF. The approximation of Lf is here computed as the application of L on $f_\gamma(x) = \langle g, \tilde{\psi}_\gamma(x,\cdot)\rangle$. Interchanging the application of L and the integration, for sufficiently smooth $\tilde{\psi}_\gamma$, gives the result. □

It is shown in [**28**] that S_γ is a regularization for computing Lf if the smoothness of e_γ is adapted to the smoothing of A and the inverse of L in the following sense

$$\lim_{\varepsilon\to 0, g^\varepsilon \to g} S_{\gamma(\varepsilon, g^\varepsilon)} g^\varepsilon = LA^\dagger g \tag{2.7}$$

if g^ε is in the range of $LA^\dagger$.

The computational efficiency of the approximate inverse heavily depends on the use of invariances. We consider again the reconstruction problem in tomography. If we chose for each reconstruction point x a special mollifier, namely $e_\gamma(x,\cdot)$, then the reconstruction kernel also depends on x, the number of values to store is then the number of reconstruction points times the number of data. If we use invariances, for example translation and rotational invariances of the Radon transform and we use these invariances to produce the mollifier we can reduce this number of values to compute and store to just the number of views per direction. The mathematical basis for this can be found in [**24**]. Here we cite the corresponding result for the combination of reconstruction and image analysis from [**28**].

THEOREM 2.4. *Let $A : X \to Y$ and $L : X \to Z$ be the two operators as above. Let*

$$\begin{aligned} T_1 &: Z \to Z \\ T_2 &: X \to X \\ T_3 &: Y \to Y \end{aligned}$$

be linear operators with

$$L^* T_1 = T_2 L^* \tag{2.8}$$

$$T_2 A^* = A^* T_3 \tag{2.9}$$

and let Ψ_γ be the solution of the auxiliary problem for a general mollifier E_γ

$$A^* \Psi_\gamma = L^* E_\gamma \; . \tag{2.10}$$

Then the solution for the special mollifier

$$e_\gamma = T_1 E_\gamma \tag{2.11}$$

is

$$\psi_\gamma = T_3 \Psi_\gamma \tag{2.12}$$

As a consequence we observe that the solution for a special mollifier fulfilling the condition $e_\gamma = T_1 E_\gamma$ can be found as

$$\langle f, e_\gamma \rangle = \langle g, T_3 \Psi_\gamma \rangle \; .$$

If for example the operators A and L are of convolution type and if we chose the mollifier e_γ also of convolution type, then the mappings T_k are all of translation type, which means that also the final reconstruction formula is of convolution type.

3. Fan - Beam Tomography and Edge Detection

The mathematical model of computerized tomography in two dimensions, for the parallel geometry, is the Radon transform, see e.g. [**35**]. It is defined as

$$\mathbf{R} f(\theta, s) = \int_{\mathbb{R}^2} f(x) \delta(s - \langle x, \theta \rangle) dx$$

where $\theta \in S^1$ is a unit vector and $s \in \mathbb{R}$. In the following we summarize a few results. The central slice theorem, or projection theorem is nothing but the formal application of the adjoint operator for fixed direction θ on $\exp(\imath s\sigma)$

$$\widehat{\mathbf{R}f}(\theta,\sigma) = (2\pi)^{1/2}\hat{f}(\sigma\theta)\ . \tag{3.1}$$

The Radon transform of a derivative is

$$\mathbf{R}\frac{\partial}{\partial x_k}f(\theta,s) = \theta_k\frac{\partial}{\partial s}\mathbf{R}f(\theta,s) \tag{3.2}$$

see e.g. [**35**], and generalizations for higher derivatives. The inversion formula for the two – dimensional Radon transform is

$$\mathbf{R}^{-1} = \frac{1}{4\pi}\mathbf{R}^*\mathbf{I}^{-1} \tag{3.3}$$

where $\mathbf{R}^*$ is the adjoint operator from L_2 to L_2 known as backprojection

$$\mathbf{R}^*g(x) = \int_{S^1} g(\theta,\langle x,\theta\rangle)d\theta$$

and the Riesz potential $\mathbf{I}^{-1}$ is defined with the Fourier transform

$$\widehat{\mathbf{I}^{-1}g}(\theta,\sigma) = |\sigma|\hat{g}(\theta,\sigma)$$

where the Fourier transform acts on the second variable.

The following invariances are well established for the Radon transform. Consider for $x \in \mathbb{R}^2$ the shift operators $T_2^x f(y) = f(y-x)$ and $T_3^{\langle x,\theta\rangle}g(\theta,s) = g(\theta,s-\langle x,\theta\rangle)$ then

$$\mathbf{R}T_2^x = T_3^{\langle x,\theta\rangle}\mathbf{R}\ . \tag{3.4}$$

Another couple of intertwining operators is found by rotation. Let U be a unitary 2×2 matrix and $D_2^U f(y) = f(Uy)$. then

$$\mathbf{R}D_2^U = D_3^U\mathbf{R} \tag{3.5}$$

where $D_3^U g(\theta,s) = g(U\theta,s)$. With $(T\mathbf{R})^* = \mathbf{R}^*T^*$ we get the relations used in Theorem 2.4. These two invariances lead for a mollifier of convolution type and independent of the directions; i.e., $e_\gamma(x,y) = E_\gamma(\|x-y\|)$, to a reconstruction kernel for determining f of convolution type, independent of the direction, namely $\psi_\gamma(x;\theta,s) = \Psi_\gamma(s-\langle x\theta\rangle)$.

THEOREM 3.1. *Let the mollifier e_γ be given as*

$$e_\gamma(x,y) = E_\gamma(\|x-y\|) \tag{3.6}$$

Then the reconstruction kernel for finding f is given as

$$\psi_\gamma(x;\theta,s) = \Psi_\gamma(s-\langle x\theta\rangle) \tag{3.7}$$

where $\Psi_\gamma(s)$ is determined as

$$\Psi_\gamma = \frac{1}{4\pi}I^{-1}\mathbf{R}E_\gamma\ . \tag{3.8}$$

PROOF. We start with the auxiliary problem and use the inversion formula for $\mathbf{R}$

$$\begin{aligned}\mathbf{R}^*\psi_\gamma &= e_\gamma \\ &= \mathbf{R}^{-1}\mathbf{R}e_\gamma \\ &= \frac{1}{4\pi}\mathbf{R}^*\mathbf{I}^{-1}\mathbf{R}e_\gamma\end{aligned}$$

hence we get

$$\psi_\gamma = \frac{1}{4\pi}\mathbf{I}^{-1}\mathbf{R}e_\gamma$$

□

In order to find a reconstruction kernel for approximating $L_k f$ where $L_k = \frac{\partial}{\partial x_k}$ we use Theorem 2.3.

THEOREM 3.2. *If we denote the reconstruction kernel for approximating f by $\tilde{\psi}_\gamma$, then the reconstruction kernel for approximating $L_k f$ is given as*

$$\psi_{k\gamma\beta}(x;\theta,s) = -\tilde{W}_\beta\big(\theta_k\tilde{\psi}'_\gamma(s - \langle x,\theta\rangle)\big) \tag{3.9}$$

where $\tilde{W}_\beta$ is the smoothing operator with $\tilde{W}_\beta L = LW_\beta$ and θ_k is the k-th component of θ.

EXAMPLE 3.3. In the following we relate the regularization parameter γ with the cut-off frequency b via

$$b = 1/\gamma\ .$$

For the smoothing of the reconstruction part we use the mollifier known from the Shepp - Logan kernel with

$$\widehat{E_b * f} = (2\pi)\widehat{e_b^1}\hat{f}$$

where

$$\widehat{e_b^1}(\xi) = (2\pi)^{-1}\mathrm{sinc}\frac{\|\xi\|\pi}{2b}\chi_{[-b,b]}(\|\xi\|) \tag{3.10}$$

and where $\chi_{[-b,b]}$ is the characteristic function of the interval $[-b,b]$; i.e., it is 1 for values between $-b$ and b and 0 otherwise. This corresponds to the reconstruction kernel

$$w_b(s) = \frac{b^2}{2\pi^3}\frac{\pi/2 - (bs)\sin(bs)}{\pi^2/4 - (bs)^2}\ . \tag{3.11}$$

For the differentiation part we choose

$$\widehat{W_\beta f} = (2\pi)\widehat{e_\beta^2}\hat{f}$$

with

$$\widehat{e_\beta^2}(\xi) = (2\pi)^{-1}\mathrm{sinc}\frac{\|\xi\|\pi}{\beta} \tag{3.12}$$

leading to a combined mollifier of the form

$$E_{\beta\gamma} = e_\gamma^1 * e_\beta^2$$

with

$$\widehat{E_{\beta\gamma}}(\xi) = (2\pi)^{-1}\mathrm{sinc}\frac{\|\xi\|\pi}{2\gamma}\mathrm{sinc}\frac{\|\xi\|\pi}{\beta}\chi_{[-\gamma,\gamma]}(\|\xi\|)$$

which is of convolution type. With the convolution theorem for Fourier transforms and the projection theorem for the Radon transform we get

$$\psi_{k\beta b}(x;\theta,s) = \theta_k\psi_{\beta b}(s - \langle x,\theta\rangle) \tag{3.13}$$

where

$$\psi_{\beta b} = \frac{1}{2\beta}\big(w_b(s+\beta) - w_b(s-\beta)\big) \tag{3.14}$$

where w_b is the kernel known from the Shepp-Logan filter, see (3.11). For

$$b = \beta = \frac{\pi}{h} \tag{3.15}$$

where h denotes the distance of the detector elements, the filter for approximating $L_k f$ at the detector points $s_\ell = \ell h$ is

$$\psi_{k,\pi/h}(s_\ell) = \theta_k\frac{1}{\pi^2 h^3}\frac{8\ell}{\left(3+4\ell^2\right)^2 - 64\ell^2}\ ,\ \ell \in \mathbb{Z}\ . \tag{3.16}$$

The divergent beam transform or X–ray transform in two dimensions also delivers line integrals, the difference to the 2D Radon transform is the parametrization. For the X–ray transform one uses the source position $a \in \Gamma$ and the direction θ of the ray

$$\mathbf{D}f(a,\theta) = \int_0^\infty f(a+t\theta)dt\ . \tag{3.17}$$

If the source is moved on a circle with radius r around the object, then one can represent the source positions as $a = r\omega(\alpha)$ where $\omega(\alpha) = (\cos\alpha,\sin\alpha)^\top$. If we parametrize the direction $\theta = \theta(\beta)$ by the angle between the line connecting source and center and the ray by the angle β where $\beta = 0$ means the ray from the source through 0, then there is the following relation between 2D X–ray transform and 2D Radon transform

$$\mathbf{D}f\big(r\omega(\alpha),\theta(\beta)\big) = \mathbf{R}f\big(\omega(\alpha+\beta-\pi/2), r\sin\beta\big)\ . \tag{3.18}$$

Formally the two transforms are related by an operator where for $V = [0, 2\pi[\times[-\arcsin 1/r, \arcsin 1/r]$ the operator $\mathbf{U}$ is defined as

$$\mathbf{U} : L_2(Z) \to L_2(V, r\sin\beta)$$

with

$$\mathbf{U}g(r\omega(\alpha), \theta(\beta)) = g(\omega(\alpha+\beta-\pi/2), r\sin\beta)\ . \tag{3.19}$$

It is an easy exercise to show that $\mathbf{U}$ is a unitary operator, hence $\mathbf{U}^*\mathbf{U} = \mathbf{I}$.

LEMMA 3.4. *Let X, Y_1, Y_2 be Hilbert spaces, $A : X \to Y_1$, $B : X \to Y_2$ linear operators and $\mathbf{U} : Y_1 \to Y_2$ be unitary with $B = \mathbf{U}A$. Then the reconstruction kernel for approximating Lf where f solves $Bf = g$ is given as*

$$\Phi_\gamma = \mathbf{U}\psi_\gamma \tag{3.20}$$

where ψ_γ is the reconstruction kernel for approximating Lf where f solves $Af = g$.

PROOF. If ψ_γ solves $A^*\psi_\gamma = L^*e_\gamma$ then we get, because of the fact that $\mathbf{U}$ is unitary

$$B^*\Phi_\gamma = A^*\mathbf{U}^*\mathbf{U}\psi_\gamma = A^*\psi_\gamma = L^*e_\gamma$$

which completes the proof. □

As a consequence it is now straightforward to calculate reconstruction kernels for the fan – beam problem. We make the usual approximations in order to have the cut – off frequency independent of the reconstruction point, see e.g. [**35**], to get the approximate inversion formula with $\psi_{\beta b}$ and $\beta = b = \pi/h$ as

$$\begin{aligned}\Big(\frac{\partial f}{\partial x_k}\Big)(x) &= \frac{r(r-1)^2}{4}\int_0^{2\pi} |a-x|^{-2} \\ &\int_{-\arcsin 1/r}^{\arcsin 1/r} \psi_{\pi/h}\big((r-1)\sin(\beta-\eta)/2\big)\omega_k(\alpha+\beta-\pi/2) \\ &\times g(\alpha,\beta)\cos\beta d\beta d\alpha\end{aligned}$$

where ω_k is the k-th component of ω and $\eta = \arcsin\big(\langle\frac{x-a}{|x-a|}, a^\perp\rangle\big)$.

In order to test the algorithm we choose the well – known Shepp – Logan phantom, where we use the densities originally given by Shepp – Logan; i.e., the skull has the value 2 and the brain has the value 1 (in contrast to many authors, where these values are lowered by 1 leading to a brain consisting of air, as in the outside of the skull). The objects inside the brain differ by 1% up to 3% to the surrounding tissue.

The number of data are $p = 800$ source positions and $q = 1024$ rays per view. The reconstruction is computed on a 1025×1025 grid.
Figure 1 shows the result of the here derived algorithm where to the data 5% noise was added. We observe that even the height of the jumps is correctly computed within the numerical approximation of the derivatives.

Then we added to the data 5% noise.

The artefacts outside the object can easily be removed by implementing the support theorem for the Radon transform stating that the object vanishes on lines parallel to θ not meeting the support of the data, see [**2**].

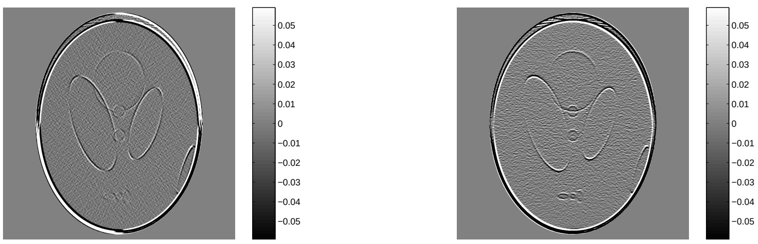

FIGURE 1: Reconstruction with the here presented algorithm for the derivative with respect to x_1(left) and x_2(right)

Figure 2 shows the result when we reconstructed in the classical way and then a smoothed derivative is applied.

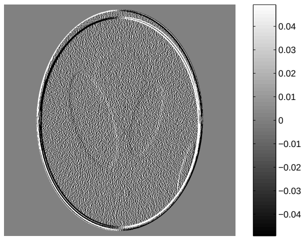

FIGURE 2: Reconstruction of the x_1 derivative with reconstruction of the density and smoothed derivative

As consequence we note that it pays off to combine the two steps of image reconstruction and image analysis wherever possible.

4. Inversion Formula for the 3D Cone Beam Transform

In the following we consider the X–ray reconstruction problem in three dimensions when the data are measured by firing an X–ray tube emitting rays to a 2D detector. The movement of the combination source – detector determines the different scanning geometries. In many real-world applications the source is moved on a circle around the object. From a mathematical point of view this has the disadvantage that the data are incomplete, the condition of Tuy-Kirillov is not fulfilled. We base our considerations on the assumption that this condition is satisfied, the reconstruction from real data nevertheless is then from the above described circular scanning geometry, because other data are not available to us so far.

A first theoretical presentation of the reconstruction kernel was given by Finch [**13**]. The use of invariance properties was a first step towards practical implementations, see [**26**]. See also the often used algorithm of Feldkamp et al. [**12**] and the contribution of Defrise and Clack [**7**]. A unified approach to those papers is contained in [**39**]. The approach of Katsevich [**19**] differs from ours in that he avoids the Crofton symbol by restricting the back projection to a range dependent on the reconstruction point x.

4.1. Mathematical model. We denote with $a \in \Gamma$ the source position, where $\Gamma \subset \mathbf{R}^3$ is a curve, and $\theta \in S^2$ is the direction of the ray. Then the cone-beam transform of a function $f \in L_2(\mathbf{R})$ is defined as

$$\mathbf{D}f(a,\theta) = \int_0^\infty f(a+t\theta)\,dt. \tag{4.1}$$

The adjoint operator as mapping from $L_2(\mathbf{R}^3) \to L_2(\Gamma \times S^2)$ is given as

$$\mathbf{D}^* g(x) = \int_\Gamma \|x-a\|^{-2}\; g\left(a, \frac{x-a}{\|x-a\|}\right) da. \tag{4.2}$$

Most attempts to find inversion formulae are based on the *Formula of Grangeat*, first published in Grangeat's PhD thesis [**14**], see also [**15**]:

$$\frac{\partial}{\partial s}\mathbf{R}f(\omega,s)\bigg|_{s=\langle a,\omega\rangle} = -\int_{S^2} \mathbf{D}f(a,\theta)\delta'(\langle\theta,\omega\rangle)\,d\theta. \tag{4.3}$$

Our starting point is now the inversion formula for the 3D Radon transform

$$f(x) = -\frac{1}{8\pi^2}\int_{S^2} \frac{\partial^2}{\partial s^2}\mathbf{R}f(\omega,s)\bigg|_{s=\langle x,\omega\rangle} d\omega, \tag{4.4}$$

that we rewrite as

$$f(x) = \frac{1}{8\pi^2}\int_{S^2}\int_{\mathbf{R}} \frac{\partial}{\partial s}\mathbf{R}f(\omega,s)\delta'(s-\langle x,\omega\rangle)\,ds\,d\omega. \tag{4.5}$$

We assume in the following that the Tuy - Kirillov condition is fulfilled. Then we can change the variables as follows: By $n(\omega,s)$ we denote the Crofton symbol, i.e. the number of source points $a \in \Gamma$ such that $\langle a,\omega\rangle = s$:

$$n(\omega,s) = \#\{a \in \Gamma : \langle a,\omega\rangle = s\}.$$

Setting $m = 1/n$, we get

$$\begin{aligned} f(x) = \frac{1}{8\pi^2} \int_{S^2} \int_\Gamma & (\mathbf{R}f)'(\omega, \langle a, \omega\rangle)\, \delta'(\langle a - x, \omega\rangle) \\ & \times |\langle \dot a, \omega\rangle|\, m(\omega, \langle a, \omega\rangle)\, da\, d\omega \\ = -\frac{1}{8\pi^2} & \int_{S^2} \int_\Gamma \int_{S^2} \mathbf{D}f(a,\theta)\, \delta'(\langle \theta, \omega\rangle)\, d\theta \\ & \times \delta'(\langle a - x, \omega\rangle)\, |\langle \dot a, \omega\rangle|\, m(\omega, \langle a, \omega\rangle)\, da\, d\omega \\ = +\frac{1}{8\pi^2} & \int_\Gamma \frac{1}{\|x-a\|^2} \int_{S^2} \int_{S^2} \mathbf{D}f(a,\theta)\, \delta'(\langle \theta, \omega\rangle)\, d\theta \\ & \times \delta'(\left\langle \frac{x-a}{\|x-a\|}, \omega \right\rangle)\ |\langle \dot a, \omega\rangle|\ m(\omega, \langle a, \omega\rangle)\, da\, d\omega \end{aligned}$$

where we used that δ' is homogeneous of degree -2 and that $\delta'(-s) = -\delta'(s)$. We now introduce the operator

$$T_1 g(\omega) = \int_{S^2} g(\theta)\, \delta'(\langle \theta, \omega\rangle)\, d\theta, \tag{4.6}$$

acting on the second variable of a function $g(a, \omega)$ as

$$T_{1,a} g(\omega) = T_1 g(a, \omega),$$

and the multiplication operator

$$M_\Gamma\, h(a, \theta) = |\langle \dot a, \omega\rangle|\ m(\omega, \langle a, \omega\rangle)\, h(\omega) \tag{4.7}$$

and state the following result, see also [**27**].

THEOREM 4.1. *Let the condition of Tuy-Kirillov be fulfilled. Then the inversion formula for the cone beam transform is given as*

$$f = \frac{1}{8\pi^2} \mathbf{D}^* T_1 M_\Gamma T_1 \mathbf{D} f$$

with the adjoint operator $\mathbf{D}^*$ of the cone beam transform and T_1 and M_Γ as defined above.

Note that both $\mathbf{D}^*$ and M_Γ depend on the scanning curve Γ, whereas T_1 only depends on the specific point a of the scanning curve.

The above theorem allows for computing reconstruction kernels. To this end we have to solve the equation

$$\mathbf{D}^* \psi_\gamma = e_\gamma,$$

in order to write the solution of $\mathbf{D} f = g$ as

$$f(x) = \langle g, \psi_\gamma(x, \cdot)\rangle_Y .$$

In the case of exact inversion, e_γ is the delta distribution, in the case of an approximate inversion formula, it is an approximation of this distribution. From the above we see that

$$\mathbf{D}^{-1} = \frac{1}{8\pi^2}\mathbf{D}^* T_1 M_\Gamma T_1$$

and we can write

$$\mathbf{D}^*\psi_\gamma = e_\gamma = \frac{1}{8\pi^2}\mathbf{D}^* T_1 M_\Gamma T_1 \mathbf{D} e_\gamma,$$

hence

$$\psi_\gamma = \frac{1}{8\pi^2} T_1 M_\Gamma T_1 \mathbf{D} e_\gamma. \tag{4.8}$$

5. Computing the reconstruction kernel

In the following, we will use (4.8) to derive an analytic formula for the reconstruction kernel in 3D. We use the Gaussian

$$e_\gamma(x,y) = (2\pi)^{-3/2}\frac{1}{\gamma^3}e^{-\frac{\|x-y\|^2}{2\gamma^2}} \tag{5.1}$$

as mollifier (which we write as $e_x(y)$) and get

$$T_1 D e_\gamma(a,\omega,x) = \frac{(2\pi)^{-1/2}}{\gamma^3}\, e^{-\frac{1}{2\gamma^2}\langle a-x,\omega\rangle^2}\, \langle a-x,\omega\rangle\,. \tag{5.2}$$

PROOF. Following [**8**, p. 69], we have

$$\int_{S^2}[Df](a,\theta)\delta'(\langle\theta,\omega\rangle)\,d\theta = -\int_{\omega^\perp}\langle[\nabla f](\langle a,\omega\rangle\,\omega + y),\omega\rangle\;dy.$$

For the Gaussian, this means

$$\begin{aligned}
[T_1 D e_x](a,\omega) &= -\int_{\omega^\perp + a}\langle[\nabla_y e_x](y),\omega\rangle\;dy\\
&= \frac{1}{\gamma^2}\left\langle\int_{\omega^\perp+a} e(\|y-x\|)(y-x)\,dy,\omega\right\rangle\\
&= \frac{(2\pi)^{-3/2}}{\gamma^5}\int_{\omega^\perp}\exp(-\frac{1}{2\gamma^2}\,\|y+z\|^2)(y+z)\,dy.
\end{aligned}$$

We introduce a rotated coordinate system, such that ω is one of the directions. As we only integrate over $\omega^\perp$, the integral reduces to an integration over $\mathbf{R}^2$ and yields the mentioned result. □

For the multiplication operator M_Γ, we need the inverse of the Crofton symbol, m. For the specific case of a circular scanning geometry, we set $n = 2$ and hence $m = 1/2$. Applying the operator T_1 to the function in (5.2) yields the following result.

THEOREM 5.1. *Let the scanning curve* Γ *be a circle with radius* R *and the density function* f *fulfills* $\operatorname{supp} f \subset r \cdot S^2, r < R$. *If the direction vector* $\theta \in S^2$ *does not lie parallel to the vector* $x - a$, *the reconstruction kernel* ψ *can be written as*

$$\begin{aligned}\psi_\gamma(a,\theta,x) = -\frac{C}{2\pi}\Bigg[\frac{p_3}{p_4}\Big\{\langle \dot{a},\theta\rangle - 2\alpha\langle a-x,\theta\rangle p_3\Big\} \\ \times \int_0^1 e^{p_1[p_2 t^2 - 1]}\,dt + p_4\langle a-x,\theta\rangle e^{p_1[p_2-1]}\Bigg],\end{aligned} \tag{5.3}$$

where

$$\begin{aligned}\alpha &= \frac{1}{2\gamma^2}, \qquad C = (2\pi)^{-3/2}\frac{1}{\gamma^3} \\ p_1 &= \alpha\left\|a - x - \langle a-x,\theta\rangle\theta\right\|^2 \\ p_2 &= \frac{\langle a - x - \langle a-x,\theta\rangle\theta, \dot{a} - \langle\dot{a},\theta\rangle\theta\rangle^2}{\left\|\dot{a} - \langle\dot{a},\theta\rangle\theta\right\|^2\left\|a - x - \langle a-x,\theta\rangle\theta\right\|^2} \\ p_3 &= \langle a - x - \langle a-x,\theta\rangle\theta, \dot{a} - \langle\dot{a},\theta\rangle\theta\rangle \\ p_4 &= \left\|\dot{a} - \langle\dot{a},\theta\rangle\theta\right\|.\end{aligned}$$

If θ *lies parallel to* $x - a$, *then the kernel can be calculated as*

$$\psi_\gamma(a,\theta,x) = -\frac{C}{2\pi}\left\|\dot{a} - \langle\dot{a},\theta\rangle\theta\right\|^2\langle a-x,\theta\rangle. \tag{5.4}$$

Theorem 5.1 provides a means for fast computations of reconstruction kernels, eliminating the need for pre-computed kernels. The calculation of the kernel took approximately 6.6 seconds on a x86 desktop system with a 3 GHz CPU, the discrete kernel has 513^2 elements.

REMARK 5.2. The circle used in theorem 5.1 does not fulfill the Tuy-Kirillov condition, hence the theorem only provides an approximative solution. With respect to the 3D Radon transform, this leads to hollow projections. In the 2D case, uniqueness is preserved, in 3D this is subject of future research. With respect to the long object problem, one additionally faces truncated projections which means that other scanning geometries, like helices are to be preferred.

6. Implementation

6.1. Invariances. As mentioned, using the approximate inverse (AI), invariances of the operator can be used to shorten the calculation of the reconstruction kernel. Using our explicit formula for ψ, we easily see the following:

(1) The reconstruction kernel depends only via $a-x$ on x, i.e. only the relative vector between a and x is important.
(2) For the point $x = 0$, we have

$$\psi_\gamma(Va, \theta, x = 0) = \psi_\gamma(a, V^{\mathtt{T}}\theta, x = 0)$$

for every rotation matrix V.

The second invariance is only true for the point $x = 0$. A first step towards a fast and easy computation of a reconstruction kernel was taken by Dietz in his PhD thesis, see [**8**]. But whereas he used a reconstruction kernel for the 3D Radon transform and subsequently calculated a numerical kernel for the ray transform, we use equation (4.8) to derive an analytical formula for the reconstruction for the X—ray transform. Using this formula, we can overcome the need for a pre-computed kernel, which gives us more flexibility.

For the approximate invariance, we define ${U_x}^{\mathtt{T}}$ to be the rotation matrix that rotates $\frac{a-x}{\|a-x\|}$ onto a/R, i.e.

$${U_x}^{\mathtt{T}} \frac{a-x}{\|a-x\|} = \frac{a}{R}.$$

For real world measurement setups, U_x will be so "close" to the identity matrix that we can then assume $U_x\dot{a} = \dot{a}$. The reason for that is that the radius of the sphere in which we reconstruct is (much) smaller than the radius of the source curve. Then, instead of calculating the reconstruction kernel for different values of x, we calculate it only for $x = 0$ and scale it by a factor of $\frac{R^2}{\|a-x\|^2}$, see [**8**]

$$\psi(a, \theta, x) \approx \frac{R^2}{\|a-x\|}\psi(a, {U_x}^{\mathtt{T}}\theta, x = 0).$$

Tying these invariances together, we see that we only need to compute the kernel once for one value of a and the different ray directions θ. The different reconstruction points x are taken into account by the simple scaling factor above.

6.2. Computational complexity. With the invariances detailed in subsection 6.1 we can implement the approximate inverse with the very same complexity as the FDK algorithm:

(1) Generate the filter matrix and calculate its Fourier transform (once!).
(2) For each source point a
    (a) Calculate the Fourier transform of the data matrix (that is, the matrix with the measured data).

(b) Multiply both matrices element-wise and calculate the inverse Fourier transform of the resulting matrix.

(3) Use these matrices for the back projection.

The only different part is the computation of the kernel 3D-matrix. As mentioned after theorem 5.1, the kernel computation takes only a few seconds, so this part is negligible. Thus, the two algorithms are on par with respect to their computational requirements.

In the following, we present reconstructions from real data, kindly provided by Fraunhofer IzfP, Saarbrücken.

FIGURE 3: Physical phantom consisting of metal

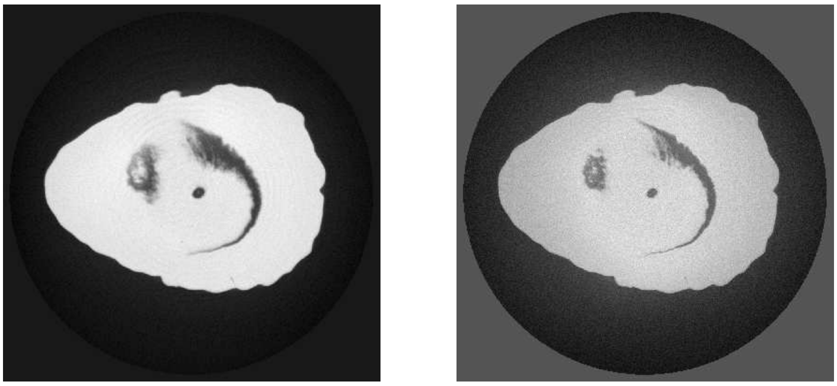

FIGURE 4: Reconstruction with the here presented algorithm (left) and with Feldkamp algorithm and Shepp Logan kernel (right).

7. Conclusion

We have presented an exact inversion formula and derived a suitable numerical inversion formula from it for the circular scanning geometry. The numerical implementation is fast enough to no longer rely on a pre-computed kernel. Instead, the kernel can be computed as part of the measurement. As such, our method has the same numerical complexity as the Feldkamp algorithm. However, the approximate inverse has both a better resolution and a lower noise level.

References

1. G. Backus and F. Gilbert *The Resolving Power of Growth Earth Data.*, Geophys. J. Roy. Astron. Soc. 16(1968), pp. 169-205
2. J. Boman and E. T. Quinto *Support theorems for real analytic Radon transforms*, Duke Math. J. 55(1987), pp. 943-948.
3. S. Bonnet, F. Peyrin, F. Turjman, and R. Prost *Multiresolution Reconstruction in Fan-Beam Tomography* IEEE Transactions on Image Processing, 11 (2002),pp. 169-176.
4. J. F. Canny *A computational approach to edge detection*, IEEE TPAMI 8 (1986), pp. 679–698.
5. B. Chalmond *Modeling and Inverse Problems in Image Analysis*, Springer, Berlin, 2003
6. M. E. Davison and F. A. Grünbaum *Tomographic reconstruction with arbitrary directions*, IEEE TNS 26 (1981), pp. 77–120

7. M. Defrise and R. Clack *A cone-beam reconstruction algorithm using shift-invariant filtering and cone-beam backprojection* IEEE Trans Med Imaging 13 (1994) pp. 186–195.
8. R. Dietz *Die approximative Inverse als Rekonstruktionsmethode in der Röntgen-Computertomographie* Ph.D. Dissertation, Saarbrücken, 1999.
9. U. Eckhardt *Zur numerischen Behandlung inkorrekt gestellter Aufgaben*, Computing 17, (1976) pp. 193–206
10. H. W. Engl, M. Hanke M and A. Neubauer *Regularization of Inverse Problems*, (Kluwer, Dordrecht, 1966
11. A. Faridani, D. V. Finch, E. L. Ritman, and K. T. Smith *Local Tomography II*, SIAM J. Appl. Math. 57 (1997), pp. 1095–1127.
12. L. Feldkamp, L. Davis and J. W. Kress *Practical cone beam algorithm* J. Opt. Soc. America, A 1 (1984), pp. 612-619.
13. D. V. Finch *Approximate reconstruction formulae for the cone beam transform I*, Preprint. 1987, available: `http://www.math.oregonstate.edu/ finch/papers/postcone.pdf`
14. P. Grangeat *Analyse d'un systéme d"'imagerie 3d par reconstuction à partir de radiographies x en géométrie conique* Ph.D. dissertation, Ecole Nationale Supérieure des Télécommunications, 1997
15. P. Grangeat *Mathematical framework of cone beam 3D reconstruction via the first derivative of the Radon transform* in: G. T. Herman, A. K. Louis and F. Natterer (eds): Mathematical methods in tomography, springer Lecture Notes in MAthematics 1991, pp. 66–97.
16. I. Hazou and D. C. Solmon *Inversion of the exponential X-ray transform. I: Analysis*, Math. Mth. Appl. Sci. 10 (1988), pp. 561–574.
17. B. Jähne *Image Processing for Scientific Applications*, CRC Press, Boca Raton, 2nd ed. 2004
18. P. Jonas and A. K. Louis *A Sobolev space analysis of linear regularization methods for ill–posed problems* J. Inv. Ill-Posed Probl. 9 (2001), pp. 59-74
19. A. Katsevich *Analysis of an exact inversion algorithm for spiral cone-beam ct* Physics in Medicine and Biology, 47 (2002) pp. 2583–2597.
20. A. Katsevich *Improved cone beam local tomography*, Inverse Problems, 22 (2006), pp. 627–643
21. A. K. Louis *Acceleration of convergence for finite element solutions of the Poisson equation*, Numer. Math. 33 (1979) pp. 43–53
22. A. K. Louis *Approximate inverse of the 3D Radon transform*, Math. Meth. Appl. Sci. 5 (1983), pp. 176–185.
23. A. K. Louis *Inverse und schlecht gestellte Probleme*, Teubner, Stuttgart, 1989.
24. A. K. Louis *Approximate inverse for linear and some nonlinear problems* Inverse Problems, 12 (1996), pp. 175-190
25. A. K. Louis *A Unified approach to regularization methods for linear ill–posed problems*, Inverse Problems, 15 (1999), pp. 489–498.
26. A. K. Louis *Filter design in three-dimensional cone beam tomography: circular scanning geometry*, Inverse Problems, 19 (2003), pp. S31-S40.
27. A. K. Louis *Development of algorithms in computerized tomography* in: G. Olafsson and E. T. Quinto: The Radon transform, Inverse Problems and Tomography, AMS PSAM 63 (2006) pp. 25–42.

28. A. K. Louis *Combining image reconstruction and image analysis with an application to 2D tomography*, SIAM J. Imaging Sciences, 2008, accepted
29. A. K. Louis and P. Maass *A mollifier method for linear operator equations of the first kind*, Inverse Problems, 6 (1990), pp. 427–440
30. A. K. Louis and P. Maass *Contour reconstruction in 3-D X—ray CT*, IEEE Transactions on Medical Imaging, 12 (1993), pp. 764–769
31. A. K. Louis, P. Maass and A. Rieder *Wavelets*, 2nd ed., Teubner, Stuttgart, 1989 and Wiley, Chichester, 1997 (English translation)
32. A. K. Louis, T. Weber and D. Theis *Computing reconstruction kernels for circular 3D cone beam tomography* IEEE Trans. Med. Imaging 2008, to appear
33. D. A. Murio *The mollification method and the numerical solution of ill-posed problems*, Wiley, Chichester, 1993
34. F. Natterer *Error bounds for Tikhonov regularization in Hilbert spaces*, Appl. Anal., 18, 29 – 37, 1984
35. F. Natterer *The mathematics of computerized tomography* , Wiley and Teubner, Stuttgart, 1986
36. F. Natterer and F. Wübbeling *Mathematical Methods in Image Reconstruction* SIAM, Philadelphia, 2001
37. S. Oeckl, T. Schön, A. Knauf and A. K. Louis *Multiresolution 3D-computerized tomography and its application to NDT*, Proc. ECNDT, 9 (2006)
38. E. T. Quinto *Radon Transforms, Differential Equations, and Microlocal Analysis*, Contemporary Mathematics, 278(2001), pp. 57-68.
39. S. Zhao, H. Yu and G. Wang *A unified framework for exact cone-beam reconstruction formulae* Medical Physics, 32 (2005) pp. 1712–1721.

INSTITUTE FOR APPLIED MATHEMATICS, SAARLAND UNIVERSITY, D-SAARBRÜCKEN, GERMANY

E-mail address: louis@num.uni-sb.de